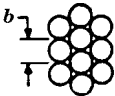
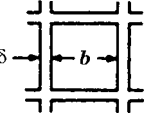
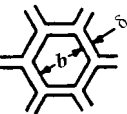
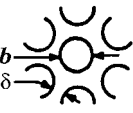
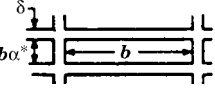



TABLE 8.2 Surface Geometrical Properties for Some Idealized Flow Passages used in Compact Regenerators

Geometry	Cell Density N_c (cells/m ²)	Porosity σ	Surface Area Density β (m ² /m ³)	Hydraulic Diameter D_h (m)
	—	0.37–0.39	$\frac{6(1-\sigma)}{b}$	$\frac{2b\sigma}{3(1-\sigma)}$
	$\frac{1}{(b+\delta)^2}$	$\frac{b^2}{(b+\delta)^2}$	$\frac{4b}{(b+\delta)^2}$	b
	$\frac{2}{\sqrt{3}(b+\delta)^2}$	$\frac{b^2}{(b+\delta)^2}$	$\frac{4b}{(b+\delta)^2}$	b
	$\frac{2}{\sqrt{3}(b+\delta)^2}$	$\frac{\pi b^2}{2\sqrt{3}(b+\delta)^2}$	$\frac{2\pi b}{\sqrt{3}(b+\delta)^2}$	b
	$\frac{1}{(b\alpha^*+\delta)(b+\delta)}$	$\frac{b^2\alpha^*}{(b\alpha^*+\delta)(b+\delta)}$	$\frac{2(1+\alpha^*)b}{(b\alpha^*+\delta)(b+\delta)}$	$\frac{2b\alpha^*}{1+\alpha^*}$
	$\frac{4\sqrt{3}}{(2b+2\delta)^2}$	$\frac{4b^2}{(2b+3\delta)^2}$	$\frac{24b}{(2b+3\delta)^2}$	$\frac{2b}{3}$

Source: Data modified from Mondt (1980).

The foregoing geometrical characteristics were used for ceramic regenerator cores of London et al. (1970). For some simple regenerator surfaces, the geometrical characteristics are summarized in Table 8.2 for completeness.

8.5 SHELL-AND-TUBE EXCHANGERS WITH SEGMENTAL BAFFLES

In this section, geometrical characteristics required for the rating and sizing of shell-and-tube exchangers with single segmental baffles are derived.

8.5.1 Tube Count

The total number of tubes in an exchanger is dependent on many geometrical variables: tube diameter, tube pitch and layout, the type of floating head, the number of tube passes, the thickness and position of pass dividers, the omission of tubes due to no-

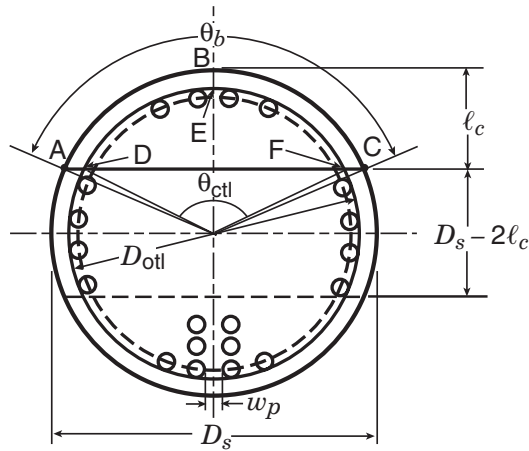


FIGURE 8.9 Nomenclature for basic baffle geometry relations for a single segmental exchanger (from Taborek, 1998).

tubes-in-window design or impingement plates, and the start of the drilling pattern relative to the shell inside diameter and pass dividers. For a fixed tubesheet design, the outermost tubes can be close to the shell inside diameter, or the diameter of the outer tube limit, D_{otl} (see Fig. 8.9), can be the largest followed by that for a split-ring floating head S (see Fig. 10.7), and D_{otl} being the smallest for a pull-through head T (see Fig. 10.5). For a U-tube bundle, some tubes are also lost near the centerline of the U-tube pattern because of the manufacturing limitations on the tube bend radius. Because of many variables involved, it is difficult to determine accurately the total number of tubes in an exchanger except for a direct count. As an alternative, the tube count may be determined approximately using published tabular values, such as those of Bell (1988), among others. For a specified diameter of the circle through the centers of the outermost tubes, D_{ctl} , the effect of the tube bundle type on the total number of tubes N_t is eliminated. Taborek (1998) provides an approximate expression for the tube count as follows in terms of D_{ctl} :

$$N_t = \begin{cases} \frac{(\pi/4)D_{ctl}^2}{C_t p_t^2} (1 - \psi_c) & \text{single tube pass} \\ \frac{(\pi/4)D_{ctl}^2}{C_t p_t^2} (1 - \psi_n) & \text{multiple tube passes} \end{cases} \quad (8.109)$$

where

$$\psi_c = \begin{cases} 0 & \text{no impingement plate} \\ \frac{\theta_{ctl}}{2\pi} - \frac{\sin \theta_{ctl}}{2\pi} & \text{impingement plate on one side} \\ 2 \left(\frac{\theta_{ctl}}{2\pi} - \frac{\sin \theta_{ctl}}{2\pi} \right) & \text{tube field removed on both sides} \end{cases} \quad (8.110)$$

ψ_n is given in Fig. 8.10, $C_t = 0.866$ for 30° and 60° tube layouts and $C_t = 1.00$ for 45° and 90° tube layout. The angle θ_{ctl} in Eq. (8.110) is in radians and is given by Eq. (8.114).

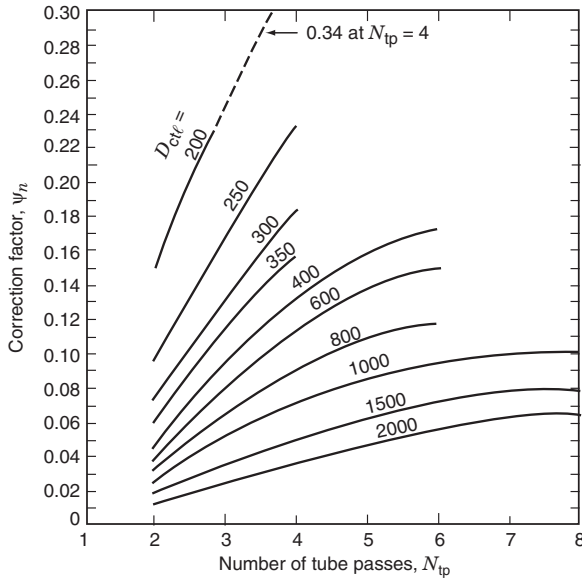


FIGURE 8.10 The correction factor ψ_n for estimation of number of tubes for tube bundles with the number of tube passes $n_p = 2 - 8$. (From Taborek, 1998.)

The accuracy in predicting tube count using Eq. (8.109) is 5% for single-tube-pass exchangers provided that large tubes are not used in relatively small shells. For multiple tube passes, the accuracy is approximately 10% for $D_s < 400$ mm and 5% for larger shell diameters.

8.5.2 Window and Crossflow Section Geometry

The single segmental E shell exchanger is one of the most common exchangers used in the process, petroleum, and power industries. The geometrical information needed for rating such an exchanger by the Bell–Delaware method (discussed in Section 9.5.1) will be derived here. The original geometry of Bell (1988) is modified based on the suggestions made by Taborek (1998). As shown in Fig. 8.11*a*, *b*, and *c*, the shell side of an E shell exchanger can be divided into three sections: internal crossflow, window, and entrance and exit sections, respectively. We calculate the necessary geometrical characteristics for window and internal crossflow sections next. The effect of larger baffle spacings at the entrance and exit sections will be included by a correction factor when we discuss the thermal design of shell-and-tube heat exchangers in Section 9.5. In addition, in this section we compute various bypass and leakage flow areas needed for the thermal design of shell-and-tube heat exchangers.

8.5.2.1 Window Section. As shown in Fig. 8.9, the gross window area (i.e., without tubes in the window) or the area of a segment ABC corresponding to the window section is

$$A_{fr,w} = \frac{\pi}{4} D_s^2 \left(\frac{\theta_b}{2\pi} - \frac{\sin \theta_b}{2\pi} \right) = \frac{D_s^2}{4} \left[\frac{\theta_b}{2} - \left(1 - \frac{2\ell_c}{D_s} \right) \sin \frac{\theta_b}{2} \right] \quad (8.111)$$

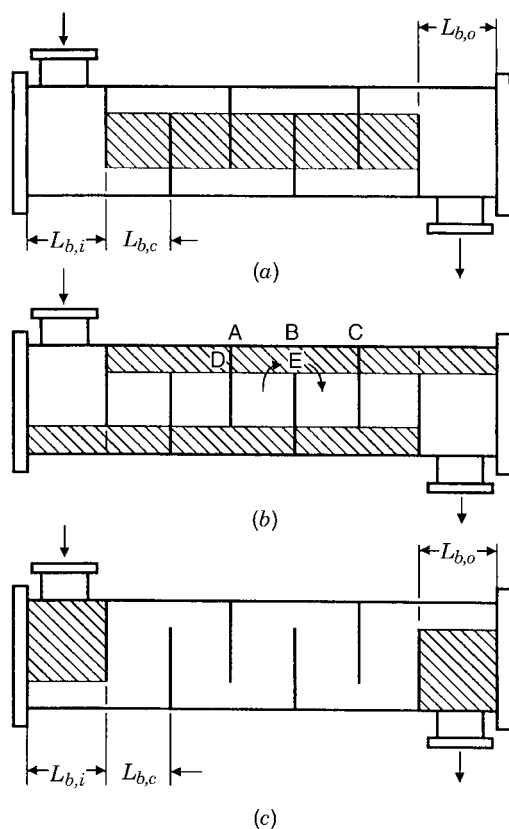


FIGURE 8.11 TEMA E shell exchanger: (a) internal cross flow sections, (b) window sections; (c) entrance and exit sections. (From Taborek, 1998.)

where θ_b is the angle in radians between two radii intersected at the inside shell wall with the baffle cut and is given by

$$\theta_b = 2 \cos^{-1} \left(1 - \frac{2\ell_c}{D_s} \right) \quad (8.112)$$

To calculate the number of tubes in the window zone, we consider the tube field uniform within the shell cross section. This idealization is violated when there are tube pass lanes (in a multipass exchanger) or when tubes are removed due to impingement plates in the nozzle entry area. We will ignore this fact and assume that it causes negligible second-order effects. Then the fraction F_w of the number of tubes in one window section encircled by the centerline of the outer tube row (Fig. 8.9) is

$$F_w = \frac{\text{area of the segment } DEF}{\text{area of the circle with } D_{\text{ctl}}} = \frac{\theta_{\text{ctl}}}{2\pi} - \frac{\sin \theta_{\text{ctl}}}{2\pi} \quad (8.113)$$

where θ_{ctl} is the angle in radians between the baffle cut and two radii of a circle through the centers of the outermost tubes (see Fig. 8.9) as follows:

$$\theta_{\text{ctl}} = 2 \cos^{-1} \left(\frac{D_s - 2\ell_c}{D_{\text{ctl}}} \right) \quad (8.114)$$

where $D_{\text{ctl}} = D_{\text{otl}} - d_o$. Consequently, the number of tubes in the window section is obtained from

$$N_{t,w} = F_w N_t \quad (8.115)$$

and the area occupied by tubes in the window section is

$$A_{\text{fr},t} = \frac{\pi}{4} d_o^2 N_{t,w} = \frac{\pi}{4} d_o^2 F_w N_t \quad (8.116)$$

The net flow area in one window section is then

$$A_{o,w} = A_{\text{fr},w} - A_{\text{fr},t} \quad (8.117)$$

where the right-hand-side terms are evaluated from Eqs. (8.111) and (8.116).

By application of the conventional definition, the hydraulic diameter of the window section of a segmental baffle is

$$D_{h,w} = \frac{4A_{o,w}}{\mathbf{P}} = \frac{4A_{o,w}}{\pi d_o N_{t,w} + \pi D_s (\theta_b/2\pi)} \quad (8.118)$$

where θ_b is given by Eq. (8.112) and \mathbf{P} is the wetted perimeter (of all tubes and the shell within the window region); the wetted perimeter of the baffle edge is usually neglected. This $D_{h,w}$ is used for shell-side pressure drop calculations in laminar flow ($\text{Re} < 100$).

The final geometrical input required for the window section is the effective number of tube rows in crossflow needed for the heat transfer and pressure drop correlations. The fluid in the window section effectively makes a 180° turn while flowing from one internal crossflow section to another. In the window region, the fluid has both crossflow and longitudinal flow components of varying magnitudes as a function of the position. Based on the visual and experimental evidence (Bell, 1963), the effective distance of penetration for crossflow in the tube field in the baffle window is about $0.4\ell_{c,\text{eff}}$ in the region AB in Fig. 8.11b while flowing away from the internal crossflow section, and about $0.4\ell_{c,\text{eff}}$ in the region BC in Fig. 8.11b while flowing toward the internal crossflow section. Here $\ell_{c,\text{eff}}$ is the distance between the baffle cut and D_{ctl} (Fig. 8.9). Hence, the number of effective tube rows in crossflow in the window section is

$$N_{r,cw} = \frac{0.8\ell_{c,\text{eff}}}{X_\ell} = \frac{0.8}{X_\ell} \left[\ell_c - \frac{1}{2}(D_s - D_{\text{ctl}}) \right] \quad (8.119)$$

8.5.2.2 Crossflow Section. The fraction F_c of the total number of tubes in the crossflow section is found from

$$F_c = 1 - 2F_w = 1 - \frac{\theta_{\text{ctl}}}{\pi} + \frac{\sin \theta_{\text{ctl}}}{\pi} \quad (8.120)$$

where the expression for F_w is obtained from Eq. (8.113). The number of tube rows $N_{r,cc}$ crossed during flow through one crossflow section between baffle tips may be obtained from a drawing or direct count or may be estimated from

$$N_{r,cc} = \frac{D_s - 2\ell_c}{X_\ell} \quad (8.121)$$

where X_ℓ is the longitudinal tube pitch summarized in Table 8.1 for various tube layouts.

The crossflow area at or near the shell centerline for one crossflow section may be estimated from

$$A_{o,cr} = \left[D_s - D_{otl} + \frac{D_{ctl}}{X_t} (X_t - d_o) \right] L_{b,c} \quad (8.122)$$

for 30° and 90° tube layout bundles. Here D_{ctl}/X_t denotes the number of $(X_t - d_o)L_{b,c}$ free-flow area in the given tube row. This equation is also valid for a 45° tube bundle having $p_t/d_o \geq 1.707$ and for a 60° tube bundle having $p_t/d_o \geq 3.732$. For 45° and 60° tube bundles having p_t/d_o lower than those indicated in the preceding line, the minimum free-flow area occurs in the diagonal spaces, and hence the term $(X_t - d_o)$ in Eq. (8.122) should be replaced by $2(p_t - d_o)$, or

$$A_{o,cr} = \left[D_s - D_{otl} + 2 \frac{D_{ctl}}{X_t} (p_t - d_o) \right] L_{b,c} \quad (8.123)$$

for 45° and 60° tube bundles. If the tubes have circular fins, the area blocked by the fins should be taken into account as in Eq. (8.36). Hence, Eq. (8.122) modifies to

$$A_{o,cr} = \left\{ D_s - D_{otl} + \frac{D_{ctl}}{X_t} [(X_t - d_o) - (d_e - d_o)\delta N_f] \right\} L_{b,c} \quad (8.124)$$

which is valid for 30° and 90° tube bundles, 45° tube bundles having $p_t/d_o \geq 1.707$, and 60° tube bundles having $p_t/d_o \geq 3.732$. For circular finned tube bundles having 45° tube layout and $p_t/d_o \leq 1.707$ or 60° tube layout and $p_t/d_o \leq 3.732$, Eq. (8.124) modifies to

$$A_{o,cr} = \left\{ D_s - D_{otl} + 2 \frac{D_{ctl}}{X_t} [p_t - d_o) - (d_e - d_o)\delta N_f] \right\} L_{b,c} \quad (8.125)$$

The number of baffles N_b is required to compute the total number of crossflow and window sections. It should be determined from the drawings or a direct count. Otherwise, compute it from the geometry of Fig. 8.11c as

$$N_b = \frac{L - L_{b,i} - L_{b,o}}{L_{b,c}} + 1 \quad (8.126)$$

where $L_{b,c}$ is the central baffle spacing, and $L_{b,i}$ and $L_{b,o}$ are the baffle spacings in the inlet and outlet regions.

8.5.3 Bypass and Leakage Flow Areas

Flow area available for bypass streams C and F (see Fig. 4.19) associated with one crossflow section, normalized with respect to the crossflow open area at or near the shell centerline, is

$$F_{bp} = \frac{A_{o,bp}}{A_{o,cr}} = \frac{(D_s - D_{otl} + 0.5N_p w_p) L_{b,c}}{A_{o,cr}} \quad (8.127)$$

where N_p is the number of pass divider lanes through the tube field that are parallel to the crossflow stream B, w_p is the width of the pass divider lane (Fig. 8.9), and $A_{o,cr}$ is given by Eqs. (8.122)–(8.125). Since the tube field is on both sides of the pass divider bypass lane, the F stream is more effective in terms of heat transfer than is the C stream. Hence, the effective bypass lane width is considered as $0.5w_p$, as indicated in Eq. (8.127).

Now let us determine the tube-to-baffle leakage area $A_{o,tb}$ for one baffle. The total number of tubes associated with one baffle is

$$N_{t,b} = N_t(1 - F_w) = N_t \left(\frac{1 + F_c}{2} \right) \quad (8.128)$$

where the value of F_w was substituted from the first equality of Eq. (8.120). If the diametral clearance (the difference between the baffle hole diameter d_1 and the tube outside diameter d_o) is δ_{tb} ($= d_1 - d_o$), the total tube-to-baffle leakage area for one baffle is

$$A_{o,tb} = \frac{\pi}{4} [(d_o + \delta_{tb})^2 - d_o^2] N_t (1 - F_w) \approx \frac{\pi d_o \delta_{tb} N_t (1 - F_w)}{2} \quad (8.129)$$

Finally, the shell-to-baffle leakage area for one baffle is associated with the gap between the shell inside diameter and the baffle. Note that this gap exists only within the sector ABC in Fig. 8.12. The shell-to-baffle leakage area

$$A_{o,sb} = \pi D_s \frac{\delta_{sb}}{2} \left(1 - \frac{\theta_b}{2\pi} \right) \quad (8.130)$$

where $\delta_{sb} = D_s - D_{baffle}$ and θ_b in radians is given by Eq. (8.112).

Example 8.3 Determine the shell-side geometrical characteristics (as outlined in Sections 8.5.2 and 8.5.3) of a 1–2 TEMA E shell-and-tube heat exchanger with a fixed tubesheet design and a 45° tube bundle with the following measured geometrical variables:

Shell-side inside diameter $D_s = 0.336$ m

Number of sealing strip pairs $N_{ss} = 1$

Tube-side outside diameter $d_o = 19.0$ mm

Total number of tubes $N_t = 102$

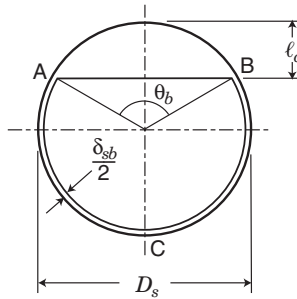


FIGURE 8.12 Single segmental baffle geometry showing shell-to-baffle diametral clearance δ_{sb} .

Tube-side inside diameter $d_i = 16.6$ mm	Transverse tube pitch $X_t = 35.4$ mm
Tube length $L = 4.3$ m	Longitudinal tube pitch $X_\ell = 17.7$ mm
Tube pitch $p_t = 25.0$ mm	Width of bypass lane $w_p = 19.0$ mm
Tube bundle layout $= 45^\circ$	Number of tube passes $n_p = 2$
Central baffle spacing $L_{b,c} = 0.279$ m	Number of pass divider lanes $N_p = 2$
Inlet baffle spacing $L_{b,i} = 0.318$ m	Diameter of the outer tube limit $D_{otl} = 0.321$ m
Outlet baffle spacing $L_{b,o} = 0.318$ m	Tube-to-baffle hole diametral clearance $\delta_{tb} = 0.794$ mm
Baffle cut $\ell_c = 86.7$ mm	Shell-to-baffle diametral clearance $\delta_{sb} = 2.946$

SOLUTION

Problem Data and Schematic: All pertinent geometrical variables for the shellside are provided above. The detailed geometry is shown in Figs. 8.9, 8.11 and 8.12.

Determine: The shell-side geometrical characteristics: baffle cut angle, fraction of total number of tubes in the window section, the area for flow through the window section, number of effective crossflow rows in each window, fraction of total number of tubes in crossflow, the number of tube rows in one crossflow section, crossflow area at or near centerline, number of baffles, fraction of crossflow area available for flow bypass, tube-to-baffle leakage area for one baffle, and shell-to-baffle leakage area for one baffle.

Assumptions: The shell-and-tube heat exchanger is assumed to have the ideal geometrical characteristics summarized in Section 8.5.

Analysis: As outlined in the text, we compute geometrical characteristics for the window section, crossflow section, and bypass and leakage flow areas.

Window Section. Let us start the calculations with computing the angle θ_b from Eq. (8.112):

$$\theta_b = 2 \cos^{-1} \left(1 - \frac{2\ell_c}{D_s} \right) = 2 \cos^{-1} \left(1 - \frac{2 \times 86.7 \times 10^{-3} \text{ m}}{0.336 \text{ m}} \right) = 2.131 \text{ rad} = 122^\circ$$

Then the gross window area $A_{fr,w}$ from Eq. (8.111) is

$$\begin{aligned} A_{fr,w} &= \frac{D_s^2}{4} \left[\frac{\theta_b}{2} - \left(1 - \frac{2\ell_c}{D_s} \right) \sin \frac{\theta_b}{2} \right] \\ &= \frac{(0.336 \text{ m})^2}{4} \left[\frac{2.131}{2} - \left(1 - \frac{2 \times 0.0867 \text{ m}}{0.336 \text{ m}} \right) \sin \frac{122^\circ}{2} \right] = 0.01813 \text{ m}^2 \end{aligned}$$

In order to calculate the fraction F_w of total tubes in the window section, first compute the baffle cut angle, using Eq. (8.114), as

$$\theta_{\text{ctl}} = 2 \cos^{-1} \left(\frac{D_s - 2\ell_c}{D_{\text{ctl}}} \right) = 2 \cos^{-1} \frac{0.336 \text{ m} - 2 \times 86.7 \times 10^{-3} \text{ m}}{0.302 \text{ m}} = 2.004 \text{ rad} = 115^\circ$$

where $D_{\text{ctl}} = D_{\text{otl}} - d_o = 0.321 \text{ m} - 19.0 \times 10^{-3} \text{ m} = 0.302 \text{ m}$. Now the fraction F_w of total tubes in the window section is given by Eq. (8.113) as

$$F_w = \frac{\theta_{\text{ctl}}}{2\pi} - \frac{\sin \theta_{\text{ctl}}}{2\pi} = \frac{2.004}{2 \times \pi} - \frac{\sin(115^\circ)}{2 \times \pi} = 0.1747$$

Consequently, the number of tubes in the window section, from Eq. (8.115), is

$$N_{t,w} = F_w N_t = 0.1747 \times 102 = 17.8$$

The area occupied by tubes in the window section, Eq. (8.116), is

$$A_{fr,t} = \frac{\pi}{4} d_o^2 F_w N_t = \frac{\pi}{4} \times (0.0190 \text{ m})^2 \times 0.1747 \times 102 = 0.00505 \text{ m}^2$$

The net flow area in one window section is then, from Eq. (8.117),

$$A_{o,w} = A_{fr,w} - A_{fr,t} = 0.01813 \text{ m}^2 - 0.00505 \text{ m}^2 = 0.01308 \text{ m}^2$$

The hydraulic diameter for the window section is given by Eq. (8.118) as

$$\begin{aligned} D_{h,w} &= \frac{4A_{o,w}}{\pi d_o N_{t,w} + \pi D_s (\theta_b / 2\pi)} \\ &= \frac{4 \times 0.01308 \text{ m}^2}{\pi \times 0.0190 \text{ m} \times 17.8 + \pi \times 0.336 \text{ m} \times (2.131 / 2\pi)} = 0.03683 \text{ m} \end{aligned}$$

Finally, the number of effective tube rows in crossflow in each window is computed using Eq. (8.119) as

$$\begin{aligned} N_{r,cw} &= \frac{0.8}{X_\ell} \left[\ell_c - \frac{1}{2} (D_s - D_{\text{ctl}}) \right] \\ &= \frac{0.8}{17.7 \times 10^{-3} \text{ m}} [86.7 \times 10^{-3} \text{ m} - (1/2)(0.336 \text{ m} - 0.302 \text{ m})] = 3.15 \approx 3 \end{aligned}$$

Crossflow Section. The fraction F_c of the total number of tubes in the crossflow section is calculated from Eq. (8.120) as

$$F_c = 1 - 2F_w = 1 - 2 \times 0.1747 = 0.6506$$

Next calculate the number of tube rows $N_{r,cc}$ crossed during flow through one crossflow section between the baffle tips [Eq. (8.121)] as

$$N_{r,cc} = \frac{D_s - 2\ell_c}{X_\ell} = \frac{0.336 \text{ m} - 2 \times 86.7 \times 10^{-3} \text{ m}}{17.7 \times 10^{-3} \text{ m}} = 9.19 \approx 9$$

The crossflow area for the 45° tube layout bundle with plain tubes at or near the shell centerline for one crossflow section can be calculated, using Eq. (8.123), as

$$\begin{aligned} A_{o,cr} &= L_{b,c} \left[D_s - D_{otl} + 2 \frac{D_{ctl}}{X_t} (p_t - d_o) \right] \\ &= 0.279 \text{ m} \times \left[0.336 \text{ m} - 0.321 \text{ m} + 2 \times \frac{0.302 \text{ m}}{0.0354 \text{ m}} \times (0.0250 \text{ m} - 0.0190 \text{ m}) \right] \\ &= 0.03275 \text{ m}^2 \end{aligned}$$

Now, compute the number of baffles from Eq. (8.126) as

$$N_b = \frac{L - L_{b,i} - L_{b,o}}{L_{b,c}} + 1 = \frac{4.3 \text{ m} - 0.318 \text{ m} - 0.318 \text{ m}}{0.279 \text{ m}} + 1 = 14.13 \approx 14$$

Bypass and Leakage Flow Areas. To calculate the fraction of crossflow area available for flow bypass, F_{bp} [Eq. (8.127)], we first have to calculate the magnitude of crossflow area for flow bypass:

$$\begin{aligned} A_{o,bp} &= L_{b,c} (D_s - D_{otl} + 0.5 N_p w_p) = 0.279 \text{ m} \times [0.336 \text{ m} - 0.321 \text{ m} + 0.5 \times 2 \times 0.0190 \text{ m}] \\ &= 0.00949 \text{ m}^2 \end{aligned}$$

Consequently,

$$F_{bp} = \frac{A_{o,bp}}{A_{o,cr}} = \frac{0.00949 \text{ m}^2}{0.03275 \text{ m}^2} = 0.2898$$

Tube-to-baffle leakage area is now given by Eq. (8.129) as follows:

$$\begin{aligned} A_{o,tb} &= \frac{\pi d_o \delta_{tb} N_t (1 - F_w)}{2} = \frac{\pi \times 0.0190 \text{ m} \times 0.000794 \text{ m} \times 102 \times (1 - 0.1747)}{2} \\ &= 0.001995 \text{ m}^2 \end{aligned}$$

Finally, the shell-to-baffle leakage area for one baffle [Eq. (8.130)] is

$$A_{o,sb} = \pi D_s \frac{\delta_{sb}}{2} \left(1 - \frac{\theta_b}{2\pi} \right) = \pi \times 0.336 \text{ m} \times \frac{0.002946 \text{ m}}{2} \left(1 - \frac{2.131}{2 \times \pi} \right) = 0.001027 \text{ m}^2$$

This concludes all geometrical characteristics needed for the thermal design/rating of a shell-and-tube heat exchanger using the Bell–Delaware method.

Discussion and Comments: The calculation procedure for computing geometrical characteristics of a shell-and-tube heat exchanger is tedious but straightforward. The same geometry has been utilized in the analysis of Example 9.4.

8.6 GASKETED PLATE HEAT EXCHANGERS

A large number of plate corrugation patterns have been developed worldwide. The chevron plate geometry (see Fig. 1.18*b* and *c*) is the most common in use today. We outline below the geometrical characteristics of the chevron plate gasketed PHE as an example by evaluating the actual heat transfer surface area due to corrugations. However, one of the common practices in industry is to ignore the effect of corrugations altogether and treat the chevron plates as if they were plain (uncorrugated) plates.

A plate with nomenclature used in the following geometrical derivations is shown in Fig. 7.28. The chevron corrugations increase surface area over the plain (uncorrugated) plate of the same outer (overall) dimensions. The ratio of the developed (actual) surface area of a chevron plate to the projected (for a plain or flat plate) is given by

$$\Phi = 1 + \frac{2}{\pi} (1 + \pi^2 \alpha^{*2})^{1/2} E(\alpha^*) \approx \frac{1}{6} (1 + \sqrt{1 + X^2} + 4\sqrt{1 + X^2/2}) \quad (8.131)$$

where $\alpha^* = 2a/\Lambda$, $E(\alpha^*)$ is the elliptical integral given in Table 7.4 with the formula for the elliptical duct, [i.e., $E(m)$], and $X = 2\pi a/\Lambda$. While the expression with the first equality is exact, Martin (1996) used the last approximate formula in Eq. (8.131) using a three-point integration method. Thus the heat transfer surface area on one fluid side of a PHE is given by

$$A = 2\Phi(WL_h + 2aL_h)N_p \approx 2\Phi WL_h N_p \quad \text{since } a \ll W \quad (8.132)$$

where W (width of the plate between gaskets) and L_h (length of the plate for heat transfer) are defined in Fig. 7.28 and N_p is the number of channels (passages) on the fluid side considered.

The free-flow area on one fluid side of a PHE is given by

$$A_o = 2aWN_p \quad (8.133)$$

Using the definition, the hydraulic diameter is given by

$$D_h = \frac{4A_o L_h}{A} = \frac{8aWN_p L_h}{2\Phi WL_h N_p} = \frac{4a}{\Phi} \quad (8.134)$$

Another commonly used set of definitions for the heat transfer surface area, free-flow area, and characteristic dimension is based on the projected surface area (i.e., as if there were no corrugations). In that case,

$$A = 2WL_h N_p \quad A_o = 2aWN_p \quad D_e = 4a \quad (8.135)$$

In this set of definitions, the characteristic dimension is referred to as an equivalent diameter, denoted by D_e . Thus,

$$D_e = \Phi D_h \quad (8.136)$$

The typical range of Φ is from 1.15 to 1.25 with $\Phi \approx 1.22$ for $\Lambda/a = 2$. This Φ can approach to 2 when Λ/a is as small as 2.46.

The total number of plates N_t in a PHE is related to the number of passes n_p and the number of channels per pass as $N_{c,p}$ as follows.

$$N_t = (n_p N_{c,p})_1 + (n_p N_{c,p})_2 + 1 \quad (8.137)$$

where the subscripts 1 and 2 refer to fluids 1 and 2. The number of thermal plates in this PHE is then $N_t - 2$. The overall height of the corrugation, $2a + \delta_p$ (where δ_p is the plate thickness) in Fig. 7.28, represents the thickness of a fully compressed gasket since the plate corrugations are in metallic contact. It can be determined as the compressed plate pack length L_{pack} (see Section 1.5.2.1 for the definition) divided by the total number of plates N_t .

The plate length for heat transfer, L_h , and that for pressure drop, L_p , are related as follows where D_p is the port diameter.

$$L_p = L_h + D_p \quad (8.138)$$

SUMMARY

Heat transfer and pressure drop correlations are highly dependent upon the geometrical characteristics of a heat transfer surface. In this chapter, the geometrical characteristics are derived for determination of heat transfer and pressure drop correlations and exchanger performance (q and Δp) of the following exchangers: tubular, tube-fin, plate-fin, regenerative and plate heat exchangers. Also pertinent geometries are derived for computing the effects of leakage and bypass flows in segmental baffle shell-and-tube exchangers. It should be emphasized that if any heat transfer or friction factor correlation from the literature is used for design and analysis of any exchanger, the geometrical characteristics *must be* evaluated in the same manner as in the original source of the correlations.

REFERENCES

- Bell, K. J., 1963, Final report of the cooperative research program on shell-and-tube heat exchangers, *Univ. Del. Eng. Exp. St. Bull.*, Vol. 5.
- Bell, K. J., 1988, Delaware method for shell-side design, in *Heat Transfer Equipment Design*, R. K. Shah, E. C. Subbarao, and R. A. Mashelkar, eds., Hemisphere Publishing, Washington, DC, pp. 227–254.
- Chang, Y. J., and C. C. Wang, 1997, A generalized heat transfer correlation for louver fin geometry, *Int. J. Heat Mass Transfer*, Vol. 40, pp. 533–544.
- Kays, W. M., and A. L. London, 1998, *Compact Heat Exchangers*, reprint 3rd ed., Krieger Publishing, Malabar, FL.
- London, A. L., M. B. O. Young, and J. H. Stang, 1970, Glass ceramic surfaces, straight triangular passages: Heat transfer and flow friction characteristics, *ASME J. Eng. Power*, Vol. 92, Ser. A, pp. 381–389.
- Martin, H., 1996, A theoretical approach to predict the performance of chevron-type plate heat exchangers, *Chem. Eng. Process.*, Vol. 35, pp. 301–310.

- Mondt, J. R., 1980, Regenerative heat exchangers: the elements of their design, selection and use, Rep. No. GMR-3396, Research Laboratories, GM Technical Center, Warren, MI,
- Sekulić, D. P., A. J. Salazar, F. Gao, J. S. Rosen, and H. S. Hatchins, 2003, Local transient behavior of a compact heat exchanger core during brazing—equivalent zonal (EZ) approach, *Int. J. Heat Exchangers*, Vol. 4, No. 1, in print.
- Shah, R. K., 1985, Compact heat exchangers, in *Handbook of Heat Transfer Applications*, 2nd ed. W. M. Rohsenow, J. P. Hartnett, and E. N. Ganić, eds., McGraw-Hill, New York., pp. 4-174 to 4-311.
- Taborek, J., 1998, Shell-and-tube heat exchangers: single phase flow, in *Handbook of Heat Exchanger Design*, G. F. Hewitt, ed., Begell House, New York, pp. 3.3.3-1 to 3.3.11-5.
- Young, M. B. O., 1969, Glass-ceramic, triangular and hexagonal passage surfaces—heat transfer and flow friction characteristics, TR HE-2, Department of Mechanical Engineering, Stanford University, Stanford, California.
- Zhao, H., and D. P. Sekulić, 2001, Brazed fin-tube joint thermal integrity vs. joint formation, *Proc. 2001 National Science Foundation Design, Service and Manufacturing Grantees and Research Conference*, Tampa, FL.; CD edition, University of Washington, Seattle, WA, DMII-998319.
- Žukauskas, A. A., 1987, Convective heat transfer in cross flow, in *Handbook of Single-Phase Convective Heat Transfer*, S. Kakaç, R. K. Shah, and W. Aung, eds., Wiley, New York, Chap. 6.

REVIEW QUESTIONS

Where multiple choices are given, circle one or more correct answers. Explain your answers briefly.

- 8.1** In a given tube bank, the actual total length of the tube used is 3 m, the tubesheets are 6 mm thick, and the blanket insulation is 150 mm (Fig. RQ8.1). The effective length of a tube for heat transfer is:
- (a) 3 m (b) 2.988 m (c) 2.838 m (d) 2.688 (e) can't tell

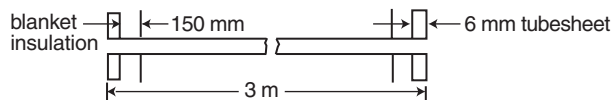


FIGURE RQ8.1

- 8.2** In Question 8.1, the effective tube length for pressure drop is:
- (a) 3 m (b) 2.988 m (c) 2.838 m (d) 2.688 (e) can't tell
- 8.3** In a tubular heat exchanger with an inline arrangement, the following geometric characteristics are of interest for in-tube heat exchanger calculations:
- (a) heat transfer area related to the header plate on the tube side
 (b) total heat transfer area
 (c) core frontal area
 (d) hydraulic diameter
- 8.4** The following surface area components are needed to evaluate primary surface area in a plate-fin heat exchanger:

- (a) total plate area (b) fin height area (c) fin base area covering plate
(d) area of side header bars
(e) area of header bars and plates at the core inlet and outlet face
- 8.5** In an offset strip fin exchanger, the secondary area consists of the:
(a) fin height area (b) fin edge height area
(c) plate area (d) header surface area
(e) fin edge width area
- 8.6** For the same b and δ (see sketches in Table 8.2 for definitions), the cell density n_c of a regenerator of square passages compared to hexagonal passages is:
(a) higher (b) the same
(c) lower (d) can't tell
- 8.7** The total number of tubes in a shell-and-tube exchanger is dependent on the:
(a) tube diameter (b) tube pitch
(c) number of tube passes (d) tube length
(e) type of floating head (f) tubesheet thickness
- 8.8** Which of the following arrangements have more tubes per pass for a specified shell inside diameter, diameter of the outer tube limit, tube outside diameter, and tube pitch?
(a) square (b) rotated square
(c) triangular (d) can't tell
- 8.9** The number of tube rows N_r in the flow direction in a crossflow zone with $D_s = 3$ m, $\ell_c = 0.675$ m, and $X_\ell = 50$ mm is approximately:
(a) 33 (b) 210 (c) 120 (d) 60 (e) none of these
- 8.10** In a no-tubes-in-window segmental baffle exchanger, the area of the window zone is:
(a) zero
(b) the area of the sector between the baffle tip and shell ID
(c) the area of the crossflow zone
(d) the bundle bypass area